Lectures on Quark Flavour Physics

Contents

1 Lecture 1: The Flavour Sector of the Standard Model **2**
1.1 What is flavour physics? 2
1.1.1 The gauge sector 2
1.1.2 The Yukawa sector 2
1.2 Interactions in the mass basis 3
1.2.1 Counting physical parameters 4
1.3 Properties of the CKM matrix 4
1.3.1 CKM unitarity and the unitarity triangle 5

2 Lecture 2: Charged Currents, EFTs, and Hadronic Matrix Elements **6**
2.1 Flavour-changing charged currents 6
2.2 The effective-field-theory expansion 7
2.3 Hadronic matrix elements 7
2.4 Processes used to extract V_{ub} and V_{cb} 9

3 Lecture 3: Neutral-Meson Mixing and CP Violation **11**
3.1 Neutral-meson mixing 11

1 Lecture 1: The Flavour Sector of the Standard Model

1.1 What is flavour physics?

Flavour physics deals with one of the puzzles in the Standard Model (SM), namely the existence of three generations of quarks and leptons with very different masses. In these lectures, we will describe how flavour comes about in the SM, which ingredients are needed to describe flavour phenomena, and some of the current problems.

We start by writing the SM Lagrangian schematically as

$$\mathcal{L}_{\mathrm{SM}} = \mathcal{L}_{\mathrm{gauge}} + \mathcal{L}_{\mathrm{Yuk}} + V(H). \tag{1.1}$$

We discuss the various terms in turn, with the exception of the Higgs potential $V(H)$.

1.1.1 The gauge sector

The gauge-sector Lagrangian is

$$\begin{aligned}\mathcal{L}_{\mathrm{gauge}} = \sum_{i=1}^{3} \sum_{\widehat{\psi}=\widehat{Q}_L,\widehat{u}_R,\widehat{d}_R,\widehat{L}_L,\widehat{e}_R} \bar{\widehat{\psi}}^{,i} i\not{D}\widehat{\psi}^{,i} - \frac{1}{4}\sum_{a=1}^{8} G^a_{\mu\nu}G^{a\mu\nu} \\ - \frac{1}{4}\sum_{a=1}^{3} W^a_{\mu\nu}W^{a\mu\nu} - \frac{1}{4}B_{\mu\nu}B^{\mu\nu}.\end{aligned} \tag{1.2}$$

The first term contains the fermionic kinetic terms, while the remaining terms are the field-strength tensors of $SU(3)_c$, $SU(2)_L$, and $U(1)_Y$.

The fermion representations are

	$SU(3)_c$	$SU(2)_L$	$U(1)_Y$	
$\widehat{Q}_L$	$\mathbf{3}$	$\mathbf{2}$	$1/6$	
$\widehat{u}_R$	$\mathbf{3}$	$\mathbf{1}$	$2/3$	quarks
$\widehat{d}_R$	$\mathbf{3}$	$\mathbf{1}$	$-1/3$	
$\widehat{L}_L$	$\mathbf{1}$	$\mathbf{2}$	$-1/2$	leptons
$\widehat{e}_R$	$\mathbf{1}$	$\mathbf{1}$	-1	

From the point of view of gauge interactions, the three generations are the same. For example, under a unitary rotation in flavour space,

$$\begin{aligned}\sum_{i=1}^{3} \bar{\widehat{Q}}_L^{,i} i\not{D}\widehat{Q}_L^{,i} \longrightarrow \sum_{i,j,k=1}^{3} \bar{\widehat{Q}}_L^{,j} (U_L^Q)^\dagger_{ji} i\not{D} (U_L^Q)_{ik}\widehat{Q}_L^{,k} \\ = \sum_{k=1}^{3} \bar{\widehat{Q}}_L^{,k} i\not{D}\widehat{Q}_L^{,k},\end{aligned} \tag{1.3}$$

and analogously for the other fields. The gauge sector is therefore invariant under independent rotations of the five fermion multiplets and has the global flavour symmetry

$$G_{\mathrm{flavour}} = U(3)^5. \tag{1.4}$$

1.1.2 The Yukawa sector

The Yukawa terms distinguish the three generations:

$$-\mathcal{L}_{\mathrm{Yuk}} = Y_d^{ij}\bar{\widehat{Q}}_L^{,i}\widehat{d}_R^{j}H + Y_u^{ij}\bar{\widehat{Q}}_L^{,i}\widehat{u}_R^{j}H^c + Y_e^{ij}\bar{\widehat{L}}_L^{,i}\widehat{e}_R^{j}H + \text{h.c.}, \tag{1.5}$$

where

$$H = \begin{pmatrix} \phi^+ \\ \phi^0 \end{pmatrix}, \qquad \langle 0|H|0\rangle = \frac{1}{\sqrt{2}}\begin{pmatrix} 0 \\ v \end{pmatrix}, \qquad H^c = i\sigma^2 H^*. \tag{1.6}$$

The Yukawa matrices $Y_{u,d,e}$ are complex 3×3 matrices. A generic flavour rotation gives, for example,

$$\bar{\widehat{Q}}{}_L^{,i}\widehat{d}_R^{j} \longrightarrow \bar{\widehat{Q}}{}_L^{,k}(U_L^Q)^\dagger_{ki}(U_R^d)_{j\ell}\widehat{d}_R^{\ell}, \tag{1.7}$$

so the Yukawa couplings break G_{flavour}.

After spontaneous symmetry breaking, in unitary gauge,

$$\widehat{Q}_L^i = \begin{pmatrix} \widehat{u}_L^i \\ \widehat{d}_L^i \end{pmatrix}, \qquad H = \frac{1}{\sqrt{2}}\begin{pmatrix} 0 \\ h+v \end{pmatrix}, \tag{1.8}$$

and therefore

$$-\mathcal{L}_{\text{Yuk}} = \frac{h+v}{\sqrt{2}}\left(Y_d^{ij}\bar{\widehat{d}}{}_L^{,i}\widehat{d}_R^{j} + Y_u^{ij}\bar{\widehat{u}}{}_L^{,i}\widehat{u}_R^{j}\right) + \text{h.c.}. \tag{1.9}$$

The terms proportional to v are mass terms. We diagonalise the two Yukawa matrices through biunitary transformations,

$$Y_d^{\text{diag}} = V_L^{d\dagger}Y_d V_R^d, \qquad Y_u^{\text{diag}} = V_L^{u\dagger}Y_u V_R^u, \tag{1.10}$$

with the field redefinitions

$$\begin{aligned} \widehat{u}_L &= V_L^u u_L, & \widehat{u}_R &= V_R^u u_R, \\ \widehat{d}_L &= V_L^d d_L, & \widehat{d}_R &= V_R^d d_R\,, \end{aligned} \tag{1.11}$$

and the matrices $V_{L,R}^{u,d}$ being separately unitary. With these transformations, the Yukawa Lagrangian becomes diagonal,

$$\mathcal{L}_{\text{Yuk}} = -\frac{h+v}{\sqrt{2}}\sum_{i=1}^{3}\left((Y_d^{\text{diag}})_{ii}\bar{d}_L^i d_R^i + (Y_u^{\text{diag}})_{ii}\bar{u}_L^i u_R^i\right) + \text{h.c.}, \tag{1.12}$$

and we identify

$$m_u = \frac{v}{\sqrt{2}}Y_u^{\text{diag}}, \qquad m_d = \frac{v}{\sqrt{2}}Y_d^{\text{diag}} \tag{1.13}$$

the mass matrices for the up and down quarks, respectively.

1.2 Interactions in the mass basis

We now examine the consequences of this rotation for the gauge interactions. The kinetic terms remain diagonal, since the unitary rotations cancel between each field and its conjugate. The same is true for neutral currents:

$$\bar{\widehat{u}}{}_L^i\gamma^\mu\widehat{u}_L^i Z_\mu = \bar{u}_L^i\gamma^\mu u_L^i Z_\mu. \tag{1.14}$$

Thus, at tree level, the SM has no flavour-changing neutral currents.

For charged-current interactions, instead,

$$\begin{aligned} \bar{\widehat{u}}{}_L^i\gamma^\mu(1-\gamma_5)\widehat{d}_L^i W_\mu^+ &\longrightarrow \bar{u}_L^i(V_L^{u\dagger})_{ik}\gamma^\mu(1-\gamma_5)(V_L^d)_{kj}d_L^j W_\mu^+ \\ &= \bar{u}_L^i\gamma^\mu(1-\gamma_5)V_{ij}d_L^j W_\mu^+, \end{aligned} \tag{1.15}$$

where

$$\boxed{V_{\text{CKM}} = V_L^{u\dagger}V_L^d} \tag{1.16}$$

is the Cabibbo–Kobayashi–Maskawa matrix [1, 2], by construction unitary, and describing flavour violation in the quark sector. In the following, we discuss how to characterise it.

1.2.1 Counting physical parameters

An $n \times n$ unitary matrix contains

$$n_\theta = \binom{n}{2} = \frac{1}{2}n(n-1) \tag{1.17}$$

rotation angles and

$$n_\phi = n^2 - n_\theta = \frac{1}{2}n(n+1) \tag{1.18}$$

phases. We are free to rephase the quark fields,

$$u_L^i \to e^{i\alpha_i} u_L^i, \qquad d_L^j \to e^{i\beta_j} d_L^j, \tag{1.19}$$

provided that the corresponding right-handed fields are rephased in the same way, so that the mass terms remain unchanged. In the charged current this is equivalent to

$$V_{ij} \to e^{i(\beta_j - \alpha_i)} V_{ij}. \tag{1.20}$$

There are $2n$ quark-field phases, but their common shift $\alpha_i \to \alpha_i + \chi$, $\beta_j \to \beta_j + \chi$ leaves the CKM matrix unchanged. It is the surviving global $U(1)$ transformation associated with baryon number. Hence only $2n - 1$ rephasings can remove phases from V, and

$$n_p = \frac{1}{2}n(n+1) - (2n-1) = \frac{1}{2}(n-1)(n-2) \tag{1.21}$$

physical phases remain. For $n = 3$, there is one physical CKM phase; for $n = 2$ there is none. The nonzero phase for three generations allows CP violation.

To summarise, tree-level FCNCs are absent, flavour-changing charged currents are proportional to CKM elements, and the six quark masses together with the four CKM parameters govern the quark-flavour sector of the SM.

1.3 Properties of the CKM matrix

The standard parametrisation uses three rotation angles and one phase. With $s_{ij} = \sin\theta_{ij}$ and $c_{ij} = \cos\theta_{ij}$,

$$V = R_{23}R_{13}(\delta)R_{12} = \begin{pmatrix} c_{12}c_{13} & s_{12}c_{13} & s_{13}e^{-i\delta} \\ -s_{12}c_{23} - c_{12}s_{23}s_{13}e^{i\delta} & c_{12}c_{23} - s_{12}s_{23}s_{13}e^{i\delta} & s_{23}c_{13} \\ s_{12}s_{23} - c_{12}c_{23}s_{13}e^{i\delta} & -c_{12}s_{23} - s_{12}c_{23}s_{13}e^{i\delta} & c_{23}c_{13} \end{pmatrix}. \tag{1.22}$$

Symbolically,

$$V = \begin{pmatrix} V_{ud} & V_{us} & V_{ub} \\ V_{cd} & V_{cs} & V_{cb} \\ V_{td} & V_{ts} & V_{tb} \end{pmatrix}. \tag{1.23}$$

The CKM elements are not parametrically independent. Numerically,

$$s_{12} \sim 0.2, \qquad s_{23} \sim 0.04, \qquad s_{13} \sim 0.004, \qquad \delta \sim 65^\circ. \tag{1.24}$$

This hierarchy motivates the Wolfenstein parametrisation [3],

$$\lambda = s_{12}, \qquad A\lambda^2 = s_{23}, \qquad A\lambda^3(\rho - i\eta) = s_{13}e^{-i\delta}, \tag{1.25}$$

for which

$$V = \begin{pmatrix} 1 - \lambda^2/2 & \lambda & A\lambda^3(\rho - i\eta) \\ -\lambda & 1 - \lambda^2/2 & A\lambda^2 \\ A\lambda^3(1 - \rho - i\eta) & -A\lambda^2 & 1 \end{pmatrix} + \mathcal{O}(\lambda^4). \tag{1.26}$$

At higher orders, it is convenient to replace the parameters ρ and η with the parameters $\bar\rho$ and $\bar\eta$, defined as

$$\bar\rho = \rho\left(1 - \frac{\lambda^2}{2}\right) + \mathcal{O}(\lambda^4), \qquad \bar\eta = \eta\left(1 - \frac{\lambda^2}{2}\right) + \mathcal{O}(\lambda^4). \tag{1.27}$$

1.3.1 CKM unitarity and the unitarity triangle

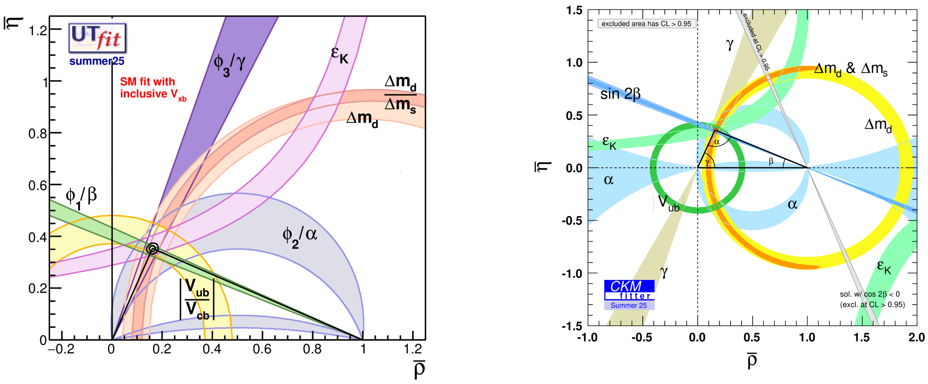

Figure 1: On the left panel we show the results from the UTfit collaboration [4], and on the right panel those from CKMfitter [5].

Unitarity of the CKM matrix implies these two sets of relations

$$\sum_{k=1}^{3} V_{ki}^* V_{ki} = 1, \qquad \sum_{k=1}^{3} V_{ki}^* V_{kj} = 0 \quad (i \neq j). \tag{1.28}$$

For the first and third columns,

$$V_{ud}^* V_{ub} + V_{cd}^* V_{cb} + V_{td}^* V_{tb} = 0. \tag{1.29}$$

Dividing by $-V_{cd}^* V_{cb}$ gives

$$-\frac{V_{ud}^* V_{ub}}{V_{cd}^* V_{cb}} - \frac{V_{td}^* V_{tb}}{V_{cd}^* V_{cb}} = 1. \tag{1.30}$$

The two complex ratios are

$$\bar\rho + i\bar\eta = -\frac{V_{ud}^* V_{ub}}{V_{cd}^* V_{cb}}, \qquad 1 - \bar\rho - i\bar\eta = -\frac{V_{td}^* V_{tb}}{V_{cd}^* V_{cb}}, \tag{1.31}$$

and can be represented as the sides of a triangle in the $(\bar\rho, \bar\eta)$ plane.

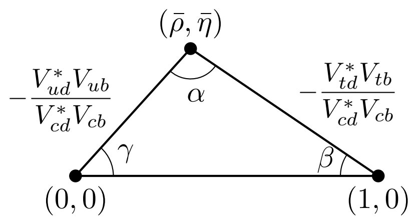

The sides and angles of the triangle are invariant under arbitrary quark-field rephasings. For example,

$$\begin{aligned}\frac{V_{ud} V_{ub}^*}{V_{cd} V_{cb}^*} &\longrightarrow \frac{V_{ud} e^{i(\beta_d - \alpha_u)} V_{ub}^* e^{-i(\beta_b - \alpha_u)}}{V_{cd} e^{i(\beta_d - \alpha_c)} V_{cb}^* e^{-i(\beta_b - \alpha_c)}} \\ &= \frac{V_{ud} V_{ub}^*}{V_{cd} V_{cb}^*}.\end{aligned} \tag{1.32}$$

Consistency checks of the unitarity triangles are performed by combining bounds from many observables. In Fig. 1 we see the results from two collaborations that perform these tests. It is evident here that consistency among observables is a key element to assess whether our current description of the flavour sector of the SM suffices. In the following, we see how to describe some of these constraints from a theoretical point of view.

2 Lecture 2: Charged Currents, EFTs, and Hadronic Matrix Elements

2.1 Flavour-changing charged currents

In the unitarity-triangle plot that we saw in the first lecture, there was another important constraint, namely the ratio $|V_{cb}/V_{ub}|$. These are the couplings appearing in

$$\mathcal{L}_W \supset \frac{g}{\sqrt{2}} V_{ib}\, \bar{u}_i \gamma^\mu P_L b\, W_\mu^+ + \text{h.c.}, \qquad i = u, c. \tag{2.1}$$

The CKM elements V_{ib} need to be determined from data, using observables whose dependence on V_{ib} is theoretically controlled. Usually, we measure V_{cb} and V_{ub} with semileptonic decays.

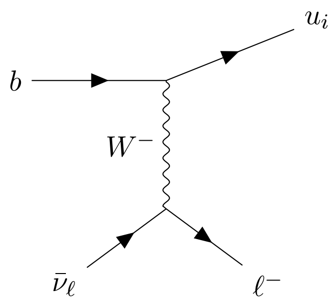

Figure 2: Feynman diagram depicting the $b \to u_i \ell \bar{\nu}$ semileptonic decay.

Semileptonic decays are described by the diagram in Fig. 2. We first look at the energy scales involved in this process. The available initial energy is m_b. This is clearly understandable if we work in the b-quark rest frame. The W is a virtual particle. When we write down the amplitude, we will have that it is proportional to the W-boson propagator,

$$\mathcal{A}(b \to u_i \ell \nu) \sim \frac{1}{q^2 - M_W^2}, \tag{2.2}$$

where q^2 is the four-momentum squared flowing into the W internal line, and it is nothing but

$$q^2 = (p_b - p_{u_i})^2. \tag{2.3}$$

From kinematics, we see that $q^2 \sim m_b^2 \ll M_W^2$. This means that we can safely neglect the q^2 term in the propagator, so that

$$\mathcal{A}(b \to u_i \ell \nu) \sim -\frac{1}{M_W^2}, \qquad q^2 \ll M_W^2. \tag{2.4}$$

From a diagrammatic point of view, the exchange of the W can therefore be replaced by the contact-interaction diagram depicted in Fig 3. This means that our process is well described by a contact interaction, modulo corrections of order q^2/M_W^2.

What is happening here is that there is an energy gap between m_b and M_W. Due to this energy gap, we can construct an effective theory where the W is not a dynamical degree of freedom anymore. Technically, we say that we have integrated out the W. At leading order, the local interaction is

$$\mathcal{L}_{\text{eff}} = -\frac{4G_F}{\sqrt{2}} V_{ib} (\bar{u}_i \gamma_\mu P_L b)(\bar{\ell} \gamma^\mu P_L \nu_\ell) + \text{h.c.}. \tag{2.5}$$

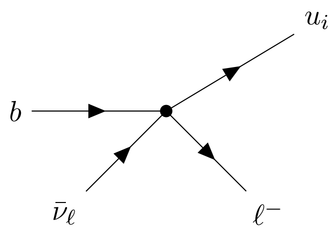

Figure 3: Feynman diagram depicting the semileptonic $b \to u_i \ell \bar{\nu}$ in the low energy effective theory.

2.2 The effective-field-theory expansion

Effective field theories, when technically introduced rigorously, are a very complicated topic. The most important point is the separation of energy scales in the problem. Formally, we perform the path integral over high-energy modes, and thereby expand the action in terms of local operators where only the light fields appear.

Alternatively to the functional approach, one can proceed in a different way. First, we list all possible gauge-invariant operators of a fixed dimension in our low-energy theory, allowed by the symmetries and the quantum numbers of the low-energy fields for a given problem:

$$\mathcal{L}_{\rm eff} = \sum_{d \geq 4} \sum_i \frac{C_i^{(d)}(\mu)}{\Lambda^{d-4}} Q_i^{(d)}(\mu). \tag{2.6}$$

The Wilson coefficients encode short-distance physics, while the matrix elements of the local operators contain the low-energy, long-distance dynamics.

For a process $i \to f$,

$$\mathcal{A}_{i \to f} \sim \sum_{d \geq 4} \sum_k \frac{C_k^{(d)}(\mu)}{\Lambda^{d-4}} \langle f | Q_k^{(d)}(\mu) | i \rangle. \tag{2.7}$$

We match the high-energy and low-energy theories by imposing

$$\langle f | \mathcal{L}_{\rm high} | i \rangle = \sum_{d \geq 4} \sum_k \frac{C_k^{(d)}(\mu)}{\Lambda^{d-4}} \langle f | Q_k^{(d)}(\mu) | i \rangle. \tag{2.8}$$

With this procedure, we obtain the Wilson coefficients at the high scale. The last step consists of running the Wilson coefficients to a different energy scale, and this is done by solving the renormalisation-group equations for the Wilson coefficients.

Let us go back to our example of semileptonic decays. In the SM there is only one operator. Where is the Wilson coefficient? Once we factor out G_F and V_{ib}, the Wilson coefficient is one at leading order. This is a particularly lucky case, but in most cases the Wilson coefficient is quite different from one.

2.3 Hadronic matrix elements

Once we have simplified our Lagrangian, there is a second aspect to be concerned about. Until now, we talked about quarks. However, the asymptotic states in QCD are not quarks, but hadrons. What we actually have to evaluate in the diagram in Fig. 4, that corresponds to the following amplitude

$$\mathcal{A} \propto \langle D^+(p_D) | \bar{c} \gamma^\mu P_L b | \bar{B}^0(p_B) \rangle. \tag{2.9}$$

A hadronic matrix element cannot be evaluated in perturbation theory. This is intuitively why. Let us take the example of a B meson. We know that it is made up of the b quark and a spectator quark, let us say the d in the case of the $\bar{B}^0$. But this is not the end of the story: the hadronic

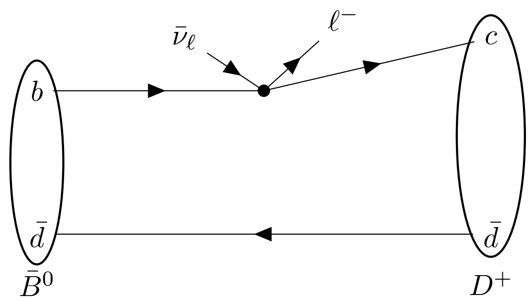

Figure 4: Diagram contributing to the $\bar{B}^0 \to D^+ \ell \bar{\nu}$ semileptonic decay.

dynamics is actually governed by a cloud made of all possible gluons and quark-antiquark pairs that are created in such a way that the net quantum numbers are carried by the valence quarks, b and $\bar{d}$. Since $m_B - m_b \sim 1\,\mathrm{GeV}$, it means that the typical energy of the sea is actually about $1\,\mathrm{GeV}$. At this energy, QCD is non-perturbative. Hence, we need non-perturbative methods to characterise hadronic matrix elements.

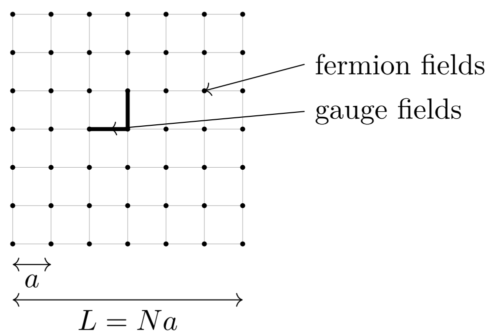

Figure 5: 2-dimensional example of discretised space-time in a finite volume.

The challenge is then to calculate hadronic matrix elements. In the case of heavy-quark physics, we usually rely on the following methods:

- **Lattice QCD**, designed to overcome this problem through a discretised space-time in a finite volume. Lattice QCD works in a box, where the sites of the grid are fermions and the links are gauge fields. The volume and lattice spacing are the regulators in a discretised quantum field theory that is now free from infinities and divergences. Of course, we have to take the continuum limit to obtain physical observables, and this precise point is currently producing systematic errors associated with this procedure.

- **QCD sum rules**, which relate the hadronic representation of a correlation function to its calculation through an OPE in an appropriate kinematic region. Quark–hadron duality is used to approximate the contribution of other hadronic states and isolate the state of interest. To illustrate the principle behind this, we start with a two-point correlation function,

$$\Pi(q^2) = i \int d^4x\, e^{iq\cdot x} \langle 0|T\{J(x)J^\dagger(0)\}|0\rangle. \tag{2.10}$$

  Inserting a complete set of hadronic states gives the hadronic representation

$$\mathbf{1} = \sum_n |n\rangle\langle n|, \qquad \rho_{\mathrm{had}}(s) = \frac{1}{\pi}\,\mathrm{Im}\,\Pi(s) = \sum_n \delta(s - m_n^2)|\langle 0|J|n\rangle|^2. \tag{2.11}$$

Analyticity yields the dispersion relation

$$\Pi(q^2) = \int_{s_{\rm th}}^{\infty} ds\, \frac{\rho_{\rm had}(s)}{s - q^2 - i0} + \text{subtractions.} \tag{2.12}$$

The same correlator is calculated using an OPE in a kinematic region where short- and long-distance dynamics can be separated. The dispersion relation puts the OPE representation in correspondence with the hadronic spectral density. Quark–hadron duality is then used to separate the state of interest from the remaining hadronic contributions, which are approximated by the partonic spectral density above an effective threshold. See [6] for a review. Depending on the process, one could also need to employ more sophisticated versions of the QCD Sum Rules such as light-cone Sum Rules.

- **Effective theories of QCD**, where we exploit a separation of scale to reduce the QCD Lagrangian. In heavy-quark physics, we employ heavy Quark Effective Theory (HQET) [7, 8], where we exploit the heavy-quark mass to expand the QCD Lagrangian in powers of $\Lambda_{\rm QCD}/m_{H_Q}$ and of α_s/π through the matching to QCD. This introduces the heavy-quark flavour symmetry, where hadrons whose light degrees of freedom have the same angular momentum and spin quantum numbers are dominated by the same non-perturbative objects.

2.4 Processes used to extract V_{ub} and V_{cb}

Representative channels are

	Exclusive	**Inclusive**
$\lvert V_{ub}\rvert$	$B \to \pi\ell\nu, \quad B_s \to K\ell\nu$	$B \to X_u\ell\nu$
$\lvert V_{cb}\rvert$	$B \to D^{(*)}\ell\nu$	$B \to X_c\ell\nu$
$\left\lvert \frac{V_{ub}}{V_{cb}} \right\rvert$	$\Lambda_b \to p\ell\nu \,/\, \Lambda_b \to \Lambda_c\ell\nu$, $B_s \to K\ell\nu \,/\, B_s \to D_s^{(*)}\ell\nu$	—

The B-meson channels are primarily studied at Belle and Belle II, whereas modes involving B_s mesons or Λ_b baryons are measured at LHCb. LHCb is not optimised to measure non-normalised quantities, for two main reasons. First of all, the initial partonic momentum is not known, and the neutrino is not detected, leaving ambiguities in the kinematics, which can be partially resolved using vertexing information. Second, one needs

$$N(B \to D\ell\nu) \propto \sigma(pp \to b\bar{b})\, f_{b\to B}\, \mathcal{B}(B \to D\ell\nu)\, \varepsilon. \tag{2.13}$$

and the cross section and fragmentation fraction are not so precisely measured. Hence, it is best to measure ratios, where some uncertainties can be cancelled out. The leptonic decay is possible at Belle II, but it still has large uncertainties. This is why, usually, V_{cb} and V_{ub} are extracted from semileptonic decays.

From the theoretical point of view, semileptonic decays imply calculating matrix elements of the type

$$\langle \ell\bar{\nu}D|\mathcal{L}_{\rm eff}|\bar{B}\rangle = -\frac{4G_F}{\sqrt{2}} V_{cb} \langle \ell\bar{\nu}|\bar{\ell}\gamma_\mu P_L \nu|0\rangle\langle D|\bar{c}\gamma^\mu P_L b|\bar{B}\rangle + \mathcal{O}(\alpha_{\rm em}). \tag{2.14}$$

At first approximation, the leptonic and hadronic matrix elements factorise. Since the W has been integrated out, there is no longer a propagating weak boson. At leading order, the leptonic and hadronic currents factorise. However, QED corrections can break this factorisation.

For a pseudoscalar-to-pseudoscalar transition,

$$\langle D(k)\,|\bar{c}\gamma^\mu b|\,\bar{B}(p)\rangle = f_+(q^2)\left[(p+k)^\mu - \frac{M_B^2 - M_D^2}{q^2}\,q^\mu\right] + f_0(q^2)\,\frac{M_B^2 - M_D^2}{q^2}\,q^\mu. \tag{2.15}$$

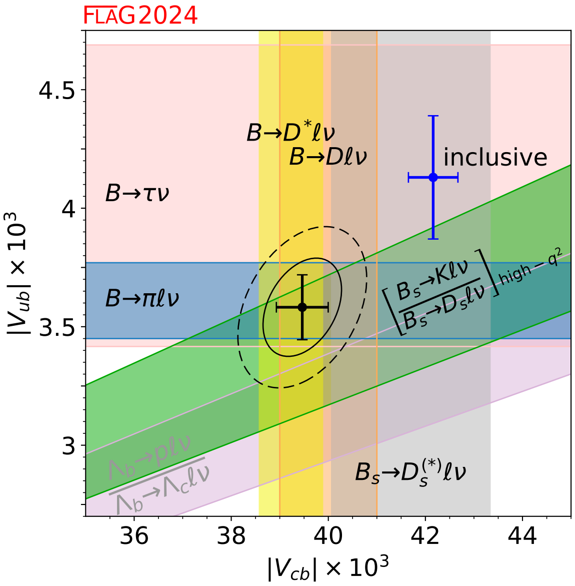

Figure 6: V_{cb} and V_{ub} plane from [9]. The black cross represents the combination of all exclusive measurements, while the blue cross is the inclusive determination.

with $q = p - k$. The functions $f_+(q^2)$ and $f_0(q^2)$ are scalar functions known as form factors, and encode the non-perturbative dynamics that governs hadronic decays. Their determination relies, hence, on the previously mentioned methods. For light charged leptons only $f_+(q^2)$ contributes to an excellent approximation. Vector final states such as D^* or ρ require several form factors and an angular analysis. In the narrow width approximation for the final vector state, in this case the D^*, we have:

$$\langle D^*(k,\eta)|\bar{c}\gamma^\mu b|\bar{B}(p)\rangle = -\epsilon^{\mu\nu\rho\sigma}\eta^*_\nu(k)\,p_\rho k_\sigma\,\frac{2V(q^2)}{M_B+M_{D^*}}, \tag{2.16}$$

$$\begin{aligned}\langle D^*(k,\eta)|\bar{c}\gamma^\mu\gamma_5 b|\bar{B}(p)\rangle = i\eta^*_\nu(k)\Bigg\{ & 2M_{D^*}A_0(q^2)\frac{q^\mu q^\nu}{q^2} \\ & + 16\frac{M_B M_{D^*}^2}{\lambda}\,A_{12}(q^2)\left[2p^\mu q^\nu - \frac{M_B^2 - M_{D^*}^2 + q^2}{q^2}q^\mu q^\nu\right] \\ & + (M_B+M_{D^*})A_1(q^2)\left[g^{\mu\nu} + \frac{2\,(M_B^2+M_{D^*}^2-q^2)}{\lambda}q^\mu q^\nu - \frac{2\,(M_B^2-M_{D^*}^2-q^2)}{\lambda}p^\mu q^\nu\right]\Bigg\}\end{aligned} \tag{2.17}$$

and η is the polarisation vector for the D^*. In the case of the D^*, the narrow width approximation is an excellent approximation. The ρ has a sizeable width, however, and the relevant hadronic object is then a multi-hadron matrix element such as $\langle\pi\pi|\bar{u}\gamma^\mu b|B\rangle$. Methods that go beyond the zero-width approximation are now being developed [10, 11].

Comparisons of inclusive and exclusive determinations reveal the longstanding V_{cb} and V_{ub} puzzles, as summarised in Fig. 6 taken from [9]. Due to recent progress, form factors for exclusive decays in Fig. 6 can be almost fully computed using lattice QCD. Inclusive determinations instead use an OPE, organised as a double expansion in α_s and inverse powers of the heavy-quark mass, and fit moments of measured distributions. New lattice methods are being developed to calculate sufficiently inclusive Euclidean observables as well, with first applications particularly relevant for inclusive determinations of V_{cb} from $B_s \to X_c\ell\bar{\nu}$ [12], albeit with large errors.

3 Lecture 3: Neutral-Meson Mixing and CP Violation

3.1 Neutral-meson mixing

Let us look at the $B^0 = d\bar{b}$, while its antiparticle is $\bar{B}^0 = \bar{d}b$. Under strong and electromagnetic interactions, B^0 and $\bar{B}^0$ are distinct flavour eigenstates. The weak interaction does not conserve flavour: we can have $B^0 \leftrightarrow \bar{B}^0$. So the B^0 and $\bar{B}^0$ differ only by their flavour quantum numbers. We saw in the previous lectures that the weak Hamiltonian does not preserve flavour. Therefore, the eigenstates of the weak Hamiltonian are not the B^0 and the $\bar{B}^0$, but a combination. This gives rise to the B^0–$\bar{B}^0$ oscillations, and to the mass difference and width difference of the two eigenstates. We formalise this. Given that this discussion holds for all neutral mesons (K^0, D^0, B^0 and B_s^0), we write it in general for a meson M^0. Most of the material is from [13], which presents a full review and a comprehensive list of measurements and observables.

The mechanism that we want to describe is the time evolution of M^0:

$$M^0(t=0) \longrightarrow P(M^0, t)\,. \tag{3.1}$$

For that, we need to write the time evolution in quantum mechanics of the M^0–$\bar{M}^0$ system. In this case, since the M^0 and $\bar{M}^0$ are unstable particles, we write down the Hamiltonian as

$$H = M - \frac{i}{2}\Gamma, \tag{3.2}$$

with

$$H = \begin{pmatrix} H_{11} & H_{12} \\ H_{21} & H_{22} \end{pmatrix} = \begin{pmatrix} \langle M^0|H|M^0\rangle & \langle M^0|H|\bar{M}^0\rangle \\ \langle \bar{M}^0|H|M^0\rangle & \langle \bar{M}^0|H|\bar{M}^0\rangle \end{pmatrix} = M - \frac{i}{2}\Gamma. \tag{3.3}$$

where M and Γ are 2×2 matrices, separately Hermitian. Here CPT invariance implies

$$M_{11} = M_{22}, \qquad \Gamma_{11} = \Gamma_{22}. \tag{3.4}$$

We can now diagonalise our system. We define

$$|M_L\rangle = p|M^0\rangle + q|\bar{M}^0\rangle, \qquad |M_H\rangle = p|M^0\rangle - q|\bar{M}^0\rangle, \qquad |p|^2 + |q|^2 = 1. \tag{3.5}$$

We call the two states light and heavy because we will associate them with the lighter and heavier eigenstates, respectively.

Now we have to diagonalise the Hamiltonian. We define some interesting quantities:

$$\Delta m = m_H - m_L, \qquad \Delta\Gamma = \Gamma_L - \Gamma_H, \tag{3.6}$$

where Δm is defined such that it is positive. Diagonalising the system, we find for the difference of the eigenvalues

$$\Delta\lambda = \lambda_H - \lambda_L = \Delta m + \frac{i}{2}\Delta\Gamma = 2\sqrt{H_{12}H_{21}}. \tag{3.7}$$

and for the mass difference and width difference,

$$(\Delta m)^2 - \frac{1}{4}(\Delta\Gamma)^2 = 4\left(|M_{12}|^2 - \frac{1}{4}|\Gamma_{12}|^2\right), \tag{3.8}$$

$$\Delta m\,\Delta\Gamma = -4\,\mathrm{Re}\,(M_{12}\Gamma_{12}^*)\,. \tag{3.9}$$

Finally, for p and q,

$$\frac{q}{p} = \frac{\Delta m - i\Delta\Gamma/2}{2M_{12} + i\Gamma_{12}}. \tag{3.10}$$

To obtain $\Delta\Gamma$ and Δm, our task is to evaluate $|M_{12}|$ and $|\Gamma_{12}|$.

With these ingredients, we can now write the time evolution:

$$|M_{H,L}(t)\rangle = e^{-iHt}|M_{H,L}(0)\rangle = e^{-i\lambda_{H,L}t}|M_{H,L}(0)\rangle. \tag{3.11}$$

since $M_{H,L}$ are eigenstates of the Hamiltonian. Now we can invert Eq. (3.5):

$$2p|M^0\rangle = |M_L\rangle + |M_H\rangle, \qquad |M^0\rangle = \frac{1}{2p}\left(|M_L\rangle + |M_H\rangle\right), \tag{3.12}$$

$$2q|\bar{M}^0\rangle = |M_L\rangle - |M_H\rangle, \qquad |\bar{M}^0\rangle = \frac{1}{2q}\left(|M_L\rangle - |M_H\rangle\right). \tag{3.13}$$

and they are valid at any t:

$$|M^0(t)\rangle = \frac{1}{2p}\left(|M_L(t)\rangle + |M_H(t)\rangle\right). \tag{3.14}$$

and, applying Eq. (3.11), we find

$$|M^0(t)\rangle = \frac{1}{2p}\left(e^{-i\lambda_L t}|M_L(0)\rangle + e^{-i\lambda_H t}|M_H(0)\rangle\right). \tag{3.15}$$

Now we re-express $|M_L(0)\rangle$ in terms of $|M^0(0)\rangle$ and $|\bar{M}^0(0)\rangle$, using Eq. (3.5):

$$\begin{aligned}|M^0(t)\rangle &= \frac{1}{2p}\Big[e^{-i\lambda_L t}(p|M^0(0)\rangle + q|\bar{M}^0(0)\rangle) \\ &\qquad + e^{-i\lambda_H t}(p|M^0(0)\rangle - q|\bar{M}^0(0)\rangle)\Big] &(3.16)\\ &= \frac{e^{-i\lambda_L t} + e^{-i\lambda_H t}}{2}|M^0(0)\rangle + \frac{q}{p}\frac{e^{-i\lambda_L t} - e^{-i\lambda_H t}}{2}|\bar{M}^0(0)\rangle. &(3.17)\end{aligned}$$

and similarly for $|\bar{M}^0(t)\rangle$. We can now use the expressions that we found before for the eigenvalues, q/p, etc., and find

$$|M^0(t)\rangle = e^{-imt}e^{-\Gamma t/2}\left[f_+(t)|M^0(0)\rangle + \frac{q}{p}f_-(t)|\bar{M}^0(0)\rangle\right], \tag{3.18}$$

$$|\bar{M}^0(t)\rangle = e^{-imt}e^{-\Gamma t/2}\left[\frac{p}{q}f_-(t)|M^0(0)\rangle + f_+(t)|\bar{M}^0(0)\rangle\right], \tag{3.19}$$

where

$$f_+(t) = \cosh\left(\frac{\Delta\Gamma t}{4}\right)\cos\left(\frac{\Delta m t}{2}\right) - i\sinh\left(\frac{\Delta\Gamma t}{4}\right)\sin\left(\frac{\Delta m t}{2}\right), \tag{3.20}$$

$$f_-(t) = -\sinh\left(\frac{\Delta\Gamma t}{4}\right)\cos\left(\frac{\Delta m t}{2}\right) + i\cosh\left(\frac{\Delta\Gamma t}{4}\right)\sin\left(\frac{\Delta m t}{2}\right). \tag{3.21}$$

From these formulae, it is evident that the two key ingredients to obtain predictions are Δm and $\Delta\Gamma$. They are linked to M_{12} and Γ_{12}. What diagrams do we need? We need the ones that transform M^0 into $\bar{M}^0$. For the sake of definiteness, we now specialise to $M^0 = B^0$. We recall from our previous lecture that at tree level there are no flavour-changing neutral currents. However, we can have them at loop order, as in Fig. 7.

Figure 7: Diagrams contributing to B^0-$\bar{B}^0$ mixing.

In particular, we have that M_{12} depends on the dispersive part of the loop, while Γ_{12} on the absorptive part of the loop. For the time being, let us focus on M_{12}. In this case, we have that we can integrate out the loop and obtain an effective Lagrangian:

$$\mathcal{L}_{\text{eff}}^{\Delta B=2} = C(\mu)Q(\mu) + \text{h.c.}, \tag{3.22}$$

with

$$Q(\mu) = \big(\bar{b}\gamma_\mu(1-\gamma_5)d\big)\big(\bar{b}\gamma^\mu(1-\gamma_5)d\big), \tag{3.23}$$

which is the only operator in the SM, and

$$C(\mu) = \frac{G_F^2 m_W^2}{16\pi^2}(V_{tb}^* V_{td})^2 S_0(x_t)\eta_B(\mu). \tag{3.24}$$

where $S_0(x_t)$ is the loop function, $x_t = m_t^2/m_W^2$, and $\eta_B(\mu)$ contains running effects. In the limit in which x_t is large, we have $S_0(x_t) \to x_t/4$. We can now directly write M_{12} as:

$$M_{12} = \frac{1}{2m_B}\langle B^0|\mathcal{L}_{\text{eff}}|\bar{B}^0\rangle. \tag{3.25}$$

We therefore need to evaluate

$$\langle B^0|\big(\bar{b}\gamma_\mu(1-\gamma_5)d\big)\big(\bar{b}\gamma^\mu(1-\gamma_5)d\big)|\bar{B}^0\rangle. \tag{3.26}$$

We insert

$$\mathbf{1} = |0\rangle\langle 0| + \sum_{n\neq 0}|n\rangle\langle n|. \tag{3.27}$$

and use the vacuum-insertion approximation, that implies neglecting all states in Eq. 3.27 apart the vacuum:

$$\begin{aligned}
&\langle B^0|\big(\bar{b}\gamma_\mu(1-\gamma_5)d\big)\big(\bar{b}\gamma^\mu(1-\gamma_5)d\big)|\bar{B}^0\rangle_{\text{VIA}} \\
&\quad = 2\langle B^0|\bar{b}\gamma_\mu(1-\gamma_5)d|0\rangle\langle 0|\bar{b}\gamma^\mu(1-\gamma_5)d|\bar{B}^0\rangle \\
&\qquad + 2\langle B^0|\bar{b}^{,i}\gamma_\mu(1-\gamma_5)d^{,j}|0\rangle\langle 0|\bar{b}^{,j}\gamma^\mu(1-\gamma_5)d^{,i}|\bar{B}^0\rangle \\
&\quad = 2\left(1+\frac{1}{N_c}\right)\langle B^0|\bar{b}\gamma_\mu(1-\gamma_5)d|0\rangle\langle 0|\bar{b}\gamma^\mu(1-\gamma_5)d|\bar{B}^0\rangle.
\end{aligned} \tag{3.28}$$

We know that this is not correct. Nowadays, we write

$$\langle B^0|Q(\mu)|\bar{B}^0\rangle = \frac{8}{3}f_B^2 m_B^2 B(\mu), \tag{3.29}$$

where $B(\mu)$ is the bag parameter, which accounts for the deviation from the vacuum-insertion approximation, and f_B and $B(\mu)$ are determined through lattice QCD.

Now, a word for Γ_{12}. In the B system, we have

$$\left|\frac{\Gamma_{12}}{M_{12}}\right| \ll 1, \tag{3.30}$$

since M_{12} is enhanced by m_t^2, whereas Γ_{12} is controlled by the scale m_b^2.

We can now look at various observables. To do so, we define the generic decay amplitudes of a B^0 to a final state f as

$$A_f = \langle f|\mathcal{L}_{\text{weak}}|B^0\rangle, \qquad \bar{A}_{\bar{f}} = \langle\bar{f}|\mathcal{L}_{\text{weak}}|\bar{B}^0\rangle, \qquad \bar{A}_f = \langle f|\mathcal{L}_{\text{weak}}|\bar{B}^0\rangle. \tag{3.31}$$

We then define

$$\lambda_f = \frac{q}{p}\frac{\bar{A}_f}{A_f}. \tag{3.32}$$

The amplitude for a B^0 meson at $t=0$ to decay to a final state f at a generic time t is:

$$\begin{aligned}\mathcal{A}(B^0(t=0)\to f(t)) &= \langle f|\mathcal{L}_{\text{weak}}|B^0(t)\rangle \\ &= e^{-imt}e^{-\Gamma t/2}\left[f_+(t)A_f+\frac{q}{p}f_-(t)\bar{A}_f\right]. \end{aligned}\tag{3.33}$$

Analogously for the $\bar{B}^0$. By putting everything together, we find

$$\begin{aligned}\Gamma(B^0(t=0)\to f(t)) = N_0|A_f|^2e^{-\Gamma t}\Bigg\{ & \frac{1+|\lambda_f|^2}{2}\cosh\left(\frac{\Delta\Gamma t}{2}\right)+\frac{1-|\lambda_f|^2}{2}\cos(\Delta m t) \\ & -\operatorname{Re}\lambda_f\sinh\left(\frac{\Delta\Gamma t}{2}\right)-\operatorname{Im}\lambda_f\sin(\Delta m t)\Bigg\}, \end{aligned}\tag{3.34}$$

$$\begin{aligned}\Gamma(\bar{B}^0(t=0)\to f(t)) = N_0|A_f|^2e^{-\Gamma t}\Bigg\{ & \frac{1+|\lambda_f|^2}{2}\cosh\left(\frac{\Delta\Gamma t}{2}\right)-\frac{1-|\lambda_f|^2}{2}\cos(\Delta m t) \\ & -\operatorname{Re}\lambda_f\sinh\left(\frac{\Delta\Gamma t}{2}\right)+\operatorname{Im}\lambda_f\sin(\Delta m t)\Bigg\}, \end{aligned}\tag{3.35}$$

where N_0 is a normalisation. We can now define:

- **direct CP violation**, if
$$|A_f|\neq|\bar{A}_{\bar{f}}|,\tag{3.36}$$
or $|A_f|\neq|\bar{A}_f|$ is f is a CP eigenstate. It does not require mixing between B^0 and $\bar{B}^0$;
- **CP violation in mixing**, if
$$\left|\frac{q}{p}\right|\neq 1.\tag{3.37}$$
- **CP violation in the interference between mixing and decay**, from the interference of
$$B^0\to f \qquad \text{and} \qquad B^0\to\bar{B}^0\to f,\tag{3.38}$$
which occurs if
$$\arg(\lambda_{\bar{f}})+\arg(\lambda_f)\neq 0.\tag{3.39}$$
For a final state that is an eigenstate of CP,
$$\operatorname{Im}\lambda_f\neq 0.\tag{3.40}$$

To conclude, we use an example of the latter: the measurement of $\sin(2\beta)$ in $B\to J/\psi K_S$. In this case, $J/\psi K_S$ is a CP eigenstate, so

$$|\bar{A}_f|=|A_f|.\tag{3.41}$$

so that $\bar{A}_f/A_f$ can only be a phase. Yet we know that, for this decay, the CKM phase is zero at leading and next-to-leading order, so that the only phase in λ_f can come from q/p. But $|q/p|=1$ if $\Gamma_{12}\simeq 0$. So we can just have CP violation in the interference, with

$$\operatorname{Im}\left(\lambda^{B_d}_{J/\psi K_S}\right)=\sin(2\beta).\tag{3.42}$$

We introduce the asymmetry

$$A_{\text{CP}}(t)=\frac{\Gamma(\bar{B}(0)\to J/\psi K_S(t))-\Gamma(B(0)\to J/\psi K_S(t))}{\Gamma(\bar{B}(0)\to J/\psi K_S(t))+\Gamma(B(0)\to J/\psi K_S(t))}=\sin(2\beta)\sin(\Delta m t).\tag{3.43}$$

Measurements of $\sin(2\beta)$ are possible using a time-dependent analysis. An example is in [14], where a measurement of $A_{\text{CP}}(t)$ is performed, enabling the extraction of $\sin(2\beta)$

References

[1] N. Cabibbo, "Unitary Symmetry and Leptonic Decays," *Phys. Rev. Lett.* **10** (1963) 531–533.

[2] M. Kobayashi and T. Maskawa, "CP-Violation in the Renormalizable Theory of Weak Interaction," *Prog. Theor. Phys.* **49** (1973) 652–657.

[3] L. Wolfenstein, "Parametrization of the Kobayashi-Maskawa Matrix," *Phys. Rev. Lett.* **51** (1983) 1945–1947.

[4] M. Bona, "Updates from UTfit beyond the Standard Model." Talk given at ichep 2026, 2026. `https://indico.cern.ch/event/1522800/contributions/6982685/`.

[5] CKMfitter Group, "Global CKM fit results, Summer 2025 update." `http://ckmfitter.in2p3.fr/www/results/plots_summer25/`, 2025.

[6] P. Colangelo and A. Khodjamirian, "QCD sum rules, a modern perspective," `arXiv:hep-ph/0010175`.

[7] H. Georgi, "An Effective Field Theory for Heavy Quarks at Low Energies," *Phys. Lett. B* **240** (1990) 447–450.

[8] M. Neubert, "Heavy-Quark Symmetry," *Phys. Rept.* **245** (1994) 259–396, `arXiv:hep-ph/9306320`.

[9] **Flavour Lattice Averaging Group (FLAG)** Collaboration, Y. Aoki *et al.*, "FLAG review 2024," *Phys. Rev. D* **113** no. 1, (2026) 014508, `arXiv:2411.04268 [hep-lat]`.

[10] L. Leskovec, S. Meinel, M. Petschlies, J. Negele, S. Paul, and A. Pochinsky, "B$\to\rho\ell\nu^-$ Resonance Form Factors from B$\to\pi\pi\ell\nu^-$ in Lattice QCD," *Phys. Rev. Lett.* **134** no. 16, (2025) 161901, `arXiv:2501.00903 [hep-lat]`.

[11] F. Erben, M. Black, P. Boyle, V. Guelpers, R. Mukherjee, A. Portelli, M. Di Carlo, M. T. Hansen, N. P. Lachini, and J. T. Tsang, "$K\pi$ scattering as a step towards $B \to K^*\ell^+\ell^-$ from Lattice QCD," *PoS* **LATTICE2025** (2026) 245, `arXiv:2603.17900 [hep-lat]`.

[12] A. De Santis *et al.*, "Inclusive $\bar{B}_s \to X_{\bar{s}c}\ell\bar{\nu}$ decays from lattice QCD: computational strategy and a first physical result," `arXiv:2607.01116 [hep-lat]`.

[13] L. Silvestrini, "Effective Theories for Quark Flavour Physics," `arXiv:1905.00798 [hep-ph]`.

[14] **LHCb** Collaboration, R. Aaij *et al.*, "Measurement of CP Violation in B0$\to\psi(\to\ell$+ℓ-)KS0($\to\pi$+π-) Decays," *Phys. Rev. Lett.* **132** no. 2, (2024) 021801, `arXiv:2309.09728 [hep-ex]`.